Bulletin of the Earthquake
Research Institute
Vol. 42 (1964), pp. 133-146

6. *Tsunami in the Vicinity of a Wave Origin* [I].

By Takao Momoi,

Earthquake Research Institute.

(Read Oct. 22, 1963.—Received Nov. 29, 1963.)

1. Introduction

The formal expression of the waves produced by a local disturbance of the bottom has already been studied by many authors. In the region of the wave origin, the numerical calculation of the theoretical expression was made by Ichiye[1] and Webb[2] for the two-dimensional case, which made the change of the generated waves clear.

On the other hand, for the three-dimensional case, the change of the waves caused by an impulse at the bottom seems still to remain obscure, though the problem was treated by several authors in a simplified form.

In the present paper we show the result obtained by numerical computation of the analytical solution without any simplification.

2. Theory

Here we take the simplest model so far as such a model does not destroy its consistency with an actual situation, since we lay stress on the explanation of the fundamental characteristics of the waves rather than on an elaborate discussion.

Assuming irrotational motion, there exists velocity potential $\phi(r, \theta, z)$ which satisfies $\Delta\phi=0$, where the three-dimensional case is treated and (r, θ)-axes are taken horizontally, with z-axis vertically downwards and the origin of the co-ordinates at the undisturbed free surface of water. The dynamic and kinematic boundary conditions at the surface $z=0$ are

$$\zeta=\frac{1}{g}\left[\frac{\partial\phi}{\partial t}+2\mu\phi\right], \tag{1}$$

1) T. Ichiye, *Jour. Ocean. Soc. Japan*, **14** (1958), 35.

2) L. M. Webb, "Theory of Waves Generated by Surface and Sea-bed Disturbances," *The Nature of Tsunamis, Appendix 1* (National Engineering Science Co. Tech. Report No. SN 57-2, 1962).

$$\frac{\partial^2\phi}{\partial t^2}+2\mu\frac{\partial\phi}{\partial t}-g\frac{\partial\phi}{\partial z}=0\,, \tag{2}$$

where t is a variable of time, μ the coefficient of virtual viscosity, g the acceleration of gravity and ζ the depression of the free surface. As the boundary condition at the bottom, we have

$$\frac{\partial\phi}{\partial z}=\eta(r,\theta,t)=f(r)\cos n\theta\cdot\chi(t)\,, \tag{3}$$

where $\eta(r,\theta,t)$ is the velocity of the bottom displacement and the separation of variables is assumed to be possible.

Using the cylindrical co-ordinates, the equation $\Delta\phi=0$ becomes

$$\left\{\frac{1}{r}\frac{\partial}{\partial r}\left(r\frac{\partial}{\partial r}\right)+\frac{1}{r^2}\frac{\partial^2}{\partial\theta^2}+\frac{\partial^2}{\partial z^2}\right\}\phi=0\,. \tag{4}$$

When a portion of the bottom is instantaneously depressed, by use of the equation and the boundary condition (1)–(4), the formal expression of ζ is already given by Sano-Hasegawa[3] and Takahasi,[4] i. e.,

$$\zeta=\cos n\theta\int_0^\infty\frac{\cos\omega t}{\cosh kH}J_n(kr)k\,dk\int_0^\infty f(\lambda)J_n(k\lambda)\lambda\,d\lambda\,, \tag{5}$$

where

$$\omega=\sqrt{gk\tanh kH}\,. \tag{6}$$

In addition to the instantaneous depression, let a portion of the bottom within a radius $r=a$ be uniformly depressed. Then, after Takahasi's paper,[5] the expression of the wave height becomes as follows:

$$\zeta=\frac{V}{\pi a}\int_0^\infty\frac{\cos\omega t}{\cosh kH}J_0(kr)J_1(ka)dk\,, \tag{7}$$

where $V=\pi a^2D_0$, V is the total volume of the depression and D_0 the displacement of a portion of the bottom.

In place of the expressions (6) and (7), the dimensionless form is preferred for universality of the computed results, i. e.,

3) K. SANO and K. HASEGAWA, *Bull. Centr. Meteor. Obs. Japan*, **2** (1929).
4) R. TAKAHASI, *Bull. Earthq. Res. Inst.*, **20** (1942), 375.
5) R. TAKAHASI, *loc. cit.*, 4).

$$\zeta_R=a^*\int_0^\infty \frac{\cos\omega^*t^*}{\cosh k^*}J_0(k^*r^*)J_1(k^*a^*)dk^*\,, \tag{8}$$

where

$$\zeta_R=\zeta^*/D_0^*=\zeta/D_0\,,$$
$$a^*=a/H\,,\quad k^*=kH\,,$$
$$D_0^*=D_0/H\,,\quad t^*=t\sqrt{g^*}\,,$$
$$g^*=g/H\,,\quad r^*=r/H\,,$$
$$\omega^*=\sqrt{k^*\tanh k^*}\,.$$

In order to calculate the expression (8), the specification of the parameter a^* is required. The entire portion of the numerical work uses the value $a^*=10$.

3. Numerical Integration

Since the analytical treatment of the integral (8) is very complicated, we have to resort to numerical evaluation. However, in this integral even numerical computation is not so easy, for the integrand fluctuates so rapidly for large values of t^*, r^*, or a^*. Therefore, a special method of integration is recommended and this might be satisfied by the method devised by Filon.[6] But, in the present stage, the calculation has been made by use of an electronic computer, following Simpson's rule. In the near future we shall make a programming of Filon's method for further study. The computer used in this study is the OKI-TAC 5090 installed at the Computation Centre of Tokyo University.

In order to apply Simpson's rule to the present problem, the finite interval of integration must be taken instead of the infinite interval of the integration (8) and we have to estimate the error for neglecting the infinite part. We have the following inequalities:

$$R_{k_0}=\left|a^*\int_{k_0}^\infty \frac{\cos\omega^*t^*}{\cosh k^*}J_0(k^*r^*)J_1(k^*a^*)\,dk^*\right|$$
$$\leq a^*\int_{k_0}^\infty 2e^{-k^*}|J_1(k^*a^*)|dk^*\,, \tag{9}$$

6) L. N. G. FILON, *Proc. Roy. Soc. Edin.*, **49** (1928-29).

where the relations

$$\left|\frac{\cos\omega^*t^*}{\cosh k^*}J_0(k^*r^*)\right|\leq\frac{1}{\cosh k^*}\leq 2e^{-k^*},$$

are used.

Putting the specified values $a^*=10$ and $k_0=10$ into the inequality (9), we have

$$R_{k_0}\leq 20\int_{10}^{\infty}e^{-k^*}|J_1(10k^*)|dk^*\,. \tag{10}$$

Since the following relation is valid to an accuracy of at least five decimal digits, i. e.,

$$\{J_1(10k^*)\}_{k^*\geq 10}\approx\left\{\sqrt{\frac{2}{\pi\cdot 10k^*}}\cos\left(10k^*-\frac{3}{4}\pi\right)\right\}_{k^*\geq 10},$$

the expression (10) becomes

$$\begin{aligned}
R_{k_0}&\leq 20\int_{10}^{\infty}e^{-k^*}\left|\sqrt{\frac{2}{\pi\cdot 10k^*}}\cos\left(10k^*-\frac{3}{4}\pi\right)\right|dk^*\\
&\leq 20\int_{10}^{\infty}e^{-k^*}\sqrt{\frac{2}{\pi\cdot 10k^*}}dk^*\\
&\leq 20\int_{10}^{\infty}e^{-k^*}\sqrt{\frac{2}{\pi\cdot 10^2}}dk^*\\
&\leq 2\sqrt{\frac{2}{\pi}}e^{-10},\\
&< 2\times 0.0000454\\
&< 0.0001\,.
\end{aligned} \tag{11}$$

The inequality (11) shows that, when we take the upper limit of the integration as 10, the integration includes an error of less than 0.0001.

In the application of Simpson's rule, the number of division is taken as 500, which prescribes a divided interval of 0.02. To check the accuracy of integration, the number of divisions of the integration is doubled, which is treated in the appendix.

4. Result of Computation

With the aid of the electronic computer, the results of the numerical computation are obtained in 10 decimal digits, but only 7 decimal digits are retained when taking the accuracy of integration into consideration.

The computed results are tabulated in Table 1 and shown graphically in Fig. 1. The numerical constant for the present model is given by $a^*=10$, which may be considered an impulse of rather small scale in view of the supposedly large scale of the area of the bottom deformation at the time of an earthquake capable of generating tsunamis. However, this model seems to give very interesting results as will be seen in the following.

The characteristic features of the waves shown in Fig. 1 are: At the moment when the impulse works at a portion of the bottom the profile of the water surface immediately matches the sea bed displacement and then the elevation changes gradually, with the height at the ring-shaped middle part decreasing (see the figures denoted by $t^*=0$ to 5 and, in the following, t^* values in the parentheses stand for those of the explanation to the figures): Thereafter, the valley of the middle part progressess in the direction of the center of the wave origin and the crest of the peripheral part spreads outwards, with the height decreasing ($t^*=6$ to 9): On arriving at the center, the ring-shaped valley gives effect to a sudden depression of the surface by about 1.5 times the magnitude of the bottom displacement, which is considered to be due to the convergence of the ring-shaped value at the central part, and then the surface of the central part gradually restores its elevation ($t^*=10$ to 15). Up to this stage, the macroscopic variation of the wave height markedly resemble that elucidated by Takahasi[7] on the basis of the shallow water approximation (the variation of the wave heights shown by Takahasi is reproduced in Fig. 2), though his theory is developed on the assumption that a portion of the bottom is elevated at the velocity $1/T$ in the finite interval T where $T=a/2c$ (a: a radius of an elevated portion of the bottom, c: a long wave velocity). But focussing a microscopic eye upon these figures, we find that several small valleys succeed the first valley and are propagated in the direction of the center in a similar way to the first valley. The variations of the succeeding small valleys (these are designated by "2nd, 3rd, 4th and 6th valley") are shown by arrows in Fig. 1. Judging

7) R. TAKAHASI, *loc. cit.*, 4).

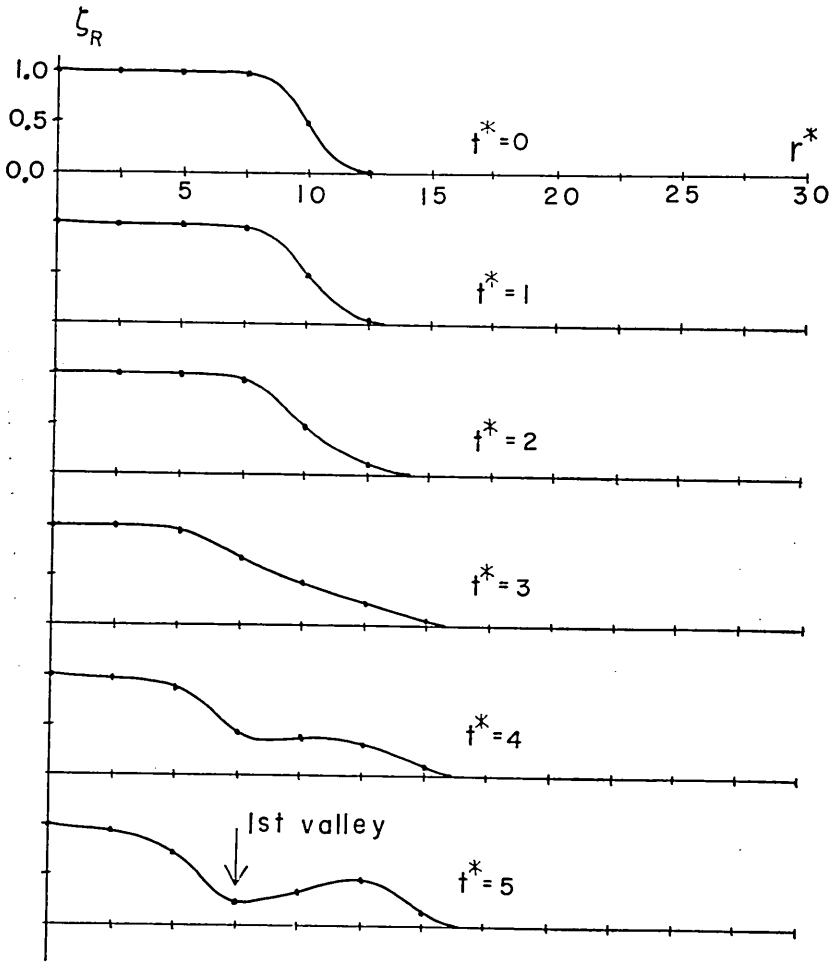

Fig. 1a.

from the results discussed by Ichiye[8] and Webb,[9] this case differs remarkably from the two-dimensional one. For two-dimensional case, the waves generated by the instantaneous and uniform elevation of a portion of the bottom, under the shallow water approximation, progress in rectangular form, while the waves computed numerically are of a very different form from the result of the shallow water approximation[8),9)].

8) T. ICHIYE, *loc. cit.*, 1).
9) L. M. WEBB, *loc. cit.*, 2).

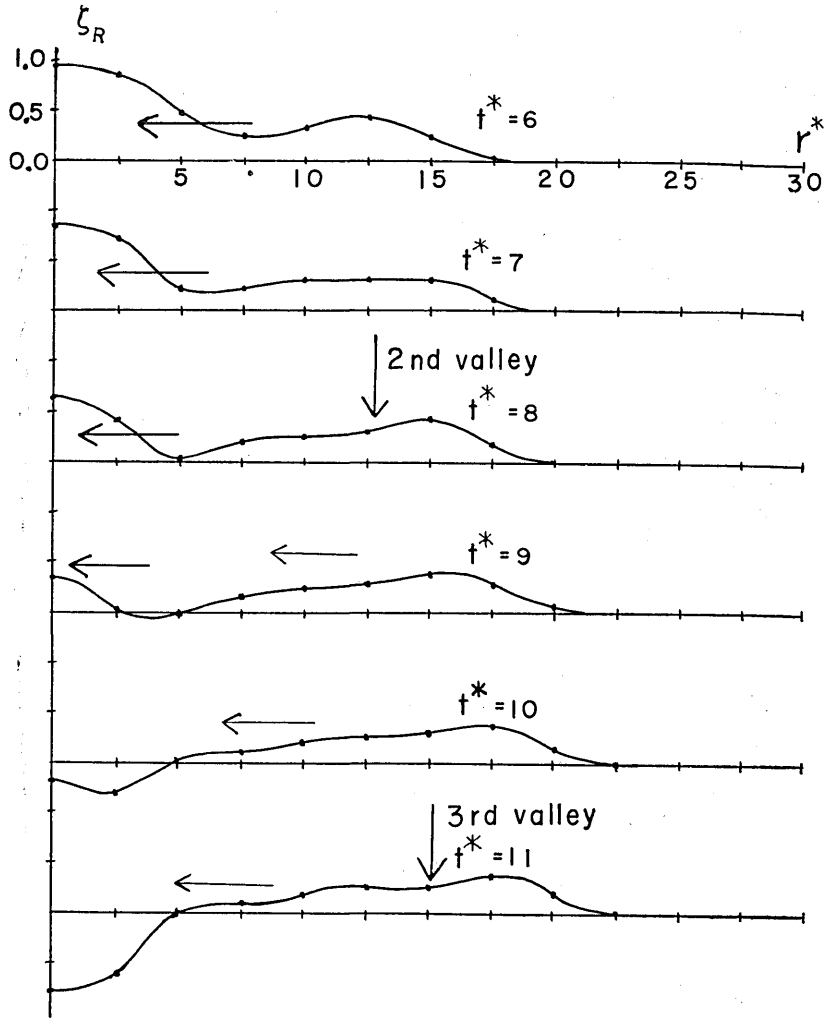

Fig. 1b.

In the later stage ($t^*>15$), the surface of the central part of the wave origin rises above the level of the mean surface, while, according to the theory based on the long wave approximation, the surface in this part is gradually elevated up to the mean surface level.

In the near future, the theoretical explanation of the succeeding

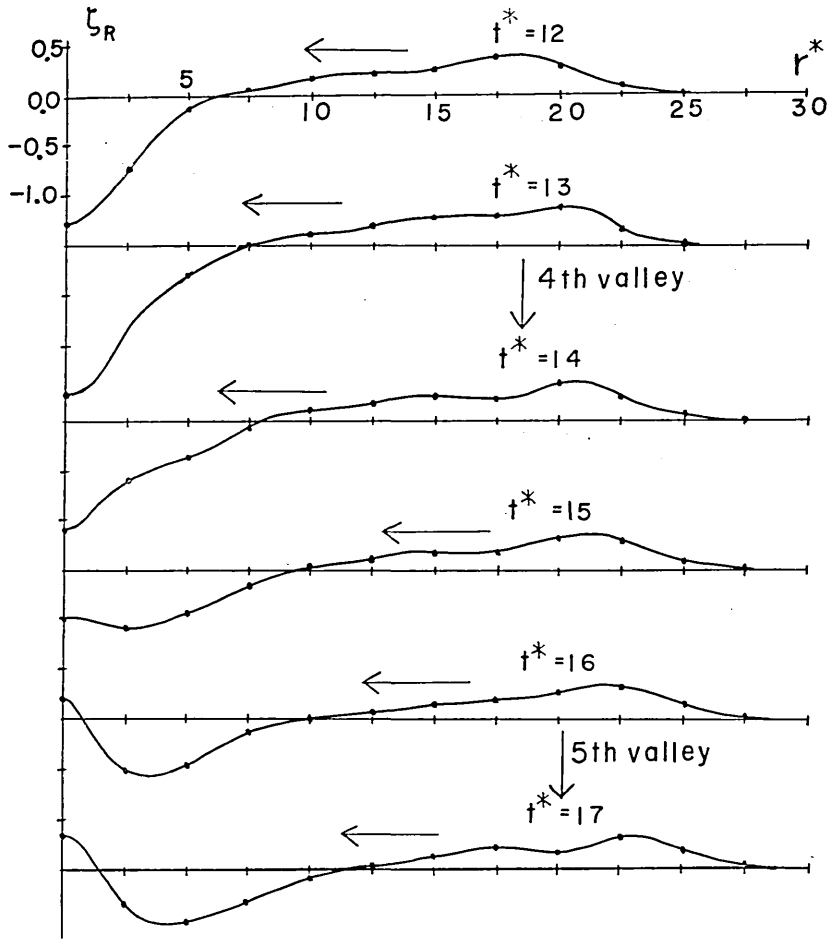

Fig. 1c.

small valleys will be given.

In the present purview, the numerical calculation is terminated at $t^*=20$, since the integration method used in this paper is too expensive and low in efficiency. In the following paper, a further calculation will be made introducing a new method.

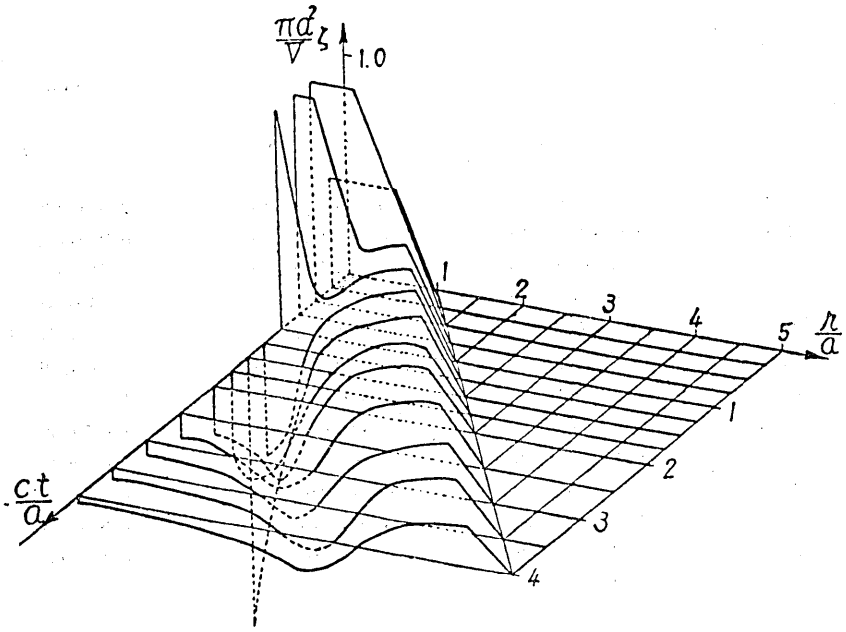

Fig. 2.

Table 1. Variation of the tsunami heights in the near field versus time.

r^*	ζ_R $(t^*=0)$	ζ_R $(t^*=1)$	ζ_R $(t^*=2)$
0.0	0.9999915×10^{0}	0.9999499×10^{0}	0.9998547×10^{0}
2.5	0.1000082×10^{1}	0.9999295×10^{0}	0.9991501×10^{0}
5.0	0.9996266×10^{0}	0.9978768×10^{0}	0.9881139×10^{0}
7.5	0.9847691×10^{0}	0.9537656×10^{0}	0.8464638×10^{0}
10.0	0.4808096×10^{0}	0.4725882×10^{0}	0.4514083×10^{0}
12.5	0.1064574×10^{-1}	0.3307119×10^{-1}	0.1084907×10^{0}
15.0	0.1482407×10^{-3}	0.1142150×10^{-2}	0.6351333×10^{-2}
17.5	0.2113268×10^{-3}	0.1385706×10^{-3}	0.1845090×10^{-3}
20.0	0.9339871×10^{-4}	0.4443158×10^{-4}	-0.9689418×10^{-5}
22.5	-0.5379959×10^{-4}	-0.2573664×10^{-4}	0.4479670×10^{-4}
25.0	-0.7364117×10^{-4}	-0.1382745×10^{-4}	0.8858811×10^{-4}
27.5	0.1286265×10^{-4}	0.3754615×10^{-4}	0.7580240×10^{-4}

(to be continued)

(continued)

r^*	ζ_R $(t^*=3)$	ζ_R $(t^*=4)$	ζ_R $(t^*=5)$
0.0	0.9992900×10^{0}	0.9961161×10^{0}	0.9843928×10^{0}
2.5	0.9959000×10^{0}	0.9841050×10^{0}	0.9494161×10^{0}
5.0	0.9552828×10^{0}	0.8731799×10^{0}	0.7148029×10^{0}
7.5	0.6520557×10^{0}	0.4226897×10^{0}	0.2696261×10^{0}
10.0	0.4247053×10^{0}	0.3980705×10^{0}	0.3724867×10^{0}
12.5	0.2393142×10^{0}	0.3820307×10^{0}	0.4535846×10^{0}
15.0	0.2334801×10^{-1}	0.6514527×10^{-1}	0.1436949×10^{0}
17.5	0.1218205×10^{-2}	0.5247607×10^{-2}	0.1659432×10^{-1}
20.0	0.7395146×10^{-4}	0.3884031×10^{-3}	0.1290088×10^{-2}
22.5	0.1168297×10^{-3}	0.1536249×10^{-3}	0.1713147×10^{-3}
25.0	0.1160648×10^{-3}	0.8096376×10^{-4}	0.7806630×10^{-4}
27.5	0.7582389×10^{-4}	0.5323416×10^{-4}	0.5963600×10^{-4}

r^*	ζ_R $(t^*=6)$	ζ_R $(t^*=7)$	ζ_R $(t^*=8)$
0.0	0.9497881×10^{0}	0.8627555×10^{0}	0.6756746×10^{0}
2.5	0.8661740×10^{0}	0.7009824×10^{0}	0.4292935×10^{0}
5.0	0.4794411×10^{0}	0.2203234×10^{0}	0.3245414×10^{-1}
7.5	0.2522872×10^{0}	0.2899782×10^{0}	0.2660130×10^{0}
10.0	0.3463485×10^{0}	0.3187166×10^{0}	0.2900711×10^{0}
12.5	0.4150260×10^{0}	0.3342798×10^{0}	0.3021926×10^{0}
15.0	0.2548433×10^{0}	0.3650360×10^{0}	0.4211717×10^{0}
17.5	0.4283568×10^{-1}	0.9311865×10^{-1}	0.1717604×10^{0}
20.0	0.4101848×10^{-2}	0.1178490×10^{-1}	0.2928900×10^{-1}
22.5	0.3195533×10^{-3}	0.9988773×10^{-3}	0.3122183×10^{-2}
25.0	0.1227699×10^{-3}	0.1524385×10^{-3}	0.2418696×10^{-3}
27.5	0.9636682×10^{-4}	0.1090638×10^{-3}	0.8350982×10^{-4}

(to be continued)

(continued)

r^*	ζ_R $(t^*=9)$	ζ_R $(t^*=10)$	ζ_R $(t^*=11)$
0.0	0.3360357×10^{0}	-0.1754016×10^{0}	-0.7899193×10^{0}
2.5	0.6368625×10^{-1}	-0.3253114×10^{0}	-0.6270651×10^{0}
5.0	-0.2061345×10^{-1}	0.1534486×10^{-1}	0.1028192×10^{-1}
7.5	0.1918454×10^{0}	0.1444428×10^{0}	0.1140192×10^{0}
10.0	0.2608218×10^{0}	0.2303534×10^{0}	0.1976970×10^{0}
12.5	0.3070566×10^{0}	0.2868599×10^{0}	0.2486277×10^{0}
15.0	0.3922706×10^{0}	0.3098178×10^{0}	0.2488740×10^{0}
17.5	0.2686923×10^{0}	0.3546836×10^{0}	0.3918923×10^{0}
22.0	0.6304801×10^{-1}	0.1185088×10^{0}	0.1948717×10^{0}
22.5	0.8549136×10^{-2}	0.2055907×10^{-1}	0.4386636×10^{-1}
25.0	0.7620756×10^{-3}	0.2412977×10^{-2}	0.6380733×10^{-2}
27.5	0.9177079×10^{-4}	0.2523557×10^{-3}	0.7300478×10^{-3}

r^*	ζ_R $(t^*=12)$	ζ_R $(t^*=13)$	ζ_R $(t^*=14)$
0.0	-0.1318866×10^{1}	-0.1504676×10^{1}	-0.1182556×10^{1}
2.5	-0.7578689×10^{0}	-0.7310744×10^{0}	-0.6485373×10^{0}
5.0	-0.1104404×10^{0}	-0.2774336×10^{0}	-0.3829539×10^{0}
7.5	0.6110017×10^{-1}	-0.2278662×10^{-2}	-0.6875528×10^{-1}
10.0	0.1623724×10^{0}	0.1240504×10^{0}	0.8172284×10^{-1}
12.5	0.2226740×10^{0}	0.1981184×10^{0}	0.1669176×10^{0}
15.0	0.2481586×10^{0}	0.2645471×10^{0}	0.2392073×10^{0}
17.5	0.3609019×10^{0}	0.2846851×10^{0}	0.2192089×10^{0}
20.0	0.2791414×10^{0}	0.3454487×10^{0}	0.3656402×10^{0}
22.5	0.8346892×10^{-1}	0.1417204×10^{0}	0.2140886×10^{0}
25.0	0.1479991×10^{-1}	0.3111060×10^{-1}	0.5958844×10^{-1}
27.5	0.1912130×10^{-2}	0.4686982×10^{-2}	0.1069126×10^{-1}

(to be continued)

(continued)

r^*	ζ_R ($t^*=15$)	ζ_R ($t^*=16$)	ζ_R ($t^*=17$)
0.0	-0.4708597×10^{0}	0.2023823×10^{0}	0.3750453×10^{0}
2.5	-0.5923625×10^{0}	-0.5279724×10^{0}	-0.3621597×10^{0}
5.0	-0.4339802×10^{0}	-0.4973813×10^{0}	-0.5395133×10^{0}
7.5	-0.1460790×10^{0}	-0.2311995×10^{0}	-0.3159732×10^{0}
10.0	0.3369226×10^{-1}	-0.2157863×10^{-1}	-0.8467500×10^{-1}
12.5	0.1337619×10^{0}	0.9757619×10^{-1}	0.5696679×10^{-1}
15.0	0.1862125×10^{0}	0.1577104×10^{0}	0.1477316×10^{0}
17.5	0.2052837×10^{0}	0.2259914×10^{0}	0.2259267×10^{0}
20.0	0.3290722×10^{0}	0.2572378×10^{0}	0.1950070×10^{0}
22.5	0.2860141×10^{0}	0.3349745×10^{0}	0.3404387×10^{0}
25.0	0.1035723×10^{0}	0.1626085×10^{0}	0.2295103×10^{0}
27.5	0.2243278×10^{-1}	0.4317091×10^{-1}	0.7618189×10^{-1}

r^*	ζ_R ($t^*=18$)	ζ_R ($t^*=19$)	ζ_R ($t^*=20$)
0.0	-0.2342108×10^{-1}	-0.5313049×10^{0}	-0.5804970×10^{0}
2.5	-0.1159223×10^{0}	0.3321555×10^{-1}	-0.4055903×10^{-1}
5.0	-0.4752243×10^{0}	-0.3270141×10^{0}	-0.1777045×10^{0}
7.5	-0.3871078×10^{0}	-0.4264374×10^{0}	-0.4163610×10^{0}
10.0	-0.1546299×10^{0}	-0.2278173×10^{0}	-0.2963416×10^{0}
12.5	0.1089761×10^{-1}	-0.4162678×10^{-1}	-0.1007081×10^{0}
15.0	0.1154557×10^{0}	0.6918237×10^{-1}	0.3351861×10^{-1}
17.5	0.1086156×10^{0}	0.1270730×10^{0}	0.1061451×10^{0}
20.0	0.1767717×10^{0}	0.1944913×10^{0}	0.2041045×10^{0}
22.5	0.2984700×10^{0}	0.2302802×10^{0}	0.1733081×10^{0}
25.0	0.2893541×10^{0}	0.3229600×10^{0}	0.3158707×10^{0}
27.5	0.1230368×10^{0}	0.1810910×10^{0}	0.2414534×10^{0}

Appendix

In order to check the accuracy of the integration, the number of the divided intervals is increased up to 1000, of which the results for time parameters $t^*=0\sim2$ and $18\sim20$ are given below:

r^*	ζ_R $(t^*=0)$	ζ_R $(t^*=1)$	ζ_R $(t^*=2)$
0.0	0.9999986×10^{0}	0.9999508×10^{0}	0.9998578×10^{0}
2.5	0.1000069×10^{1}	0.9999233×10^{0}	0.9991533×10^{0}
5.0	0.9996267×10^{0}	0.9978756×10^{0}	0.9998572×10^{0}
7.5	0.9847670×10^{0}	0.9537597×10^{0}	0.8464524×10^{0}
10.0	0.4808975×10^{0}	0.4725898×10^{0}	0.4514086×10^{0}
12.5	0.1063585×10^{-1}	0.3305881×10^{-1}	0.1084791×10^{0}
15.0	0.1482249×10^{-3}	0.1140797×10^{-2}	0.6358564×10^{-2}
17.5	0.2111355×10^{-3}	0.1385797×10^{-3}	0.1846520×10^{-3}
20.0	0.9337654×10^{-4}	0.4444547×10^{-4}	-0.9684521×10^{-5}
22.5	-0.5372119×10^{-4}	-0.2571132×10^{-4}	0.4474011×10^{-4}
25.0	-0.7367899×10^{-4}	-0.1389768×10^{-4}	0.8896721×10^{-4}
27.5	0.1287659×10^{-4}	0.3756298×10^{-4}	0.7582419×10^{-4}

r^*	ζ_R $(t^*=18)$	ζ_R $(t^*=19)$	ζ_R $(t^*=20)$
0.0	-0.2347102×10^{-1}	-0.5313474×10^{0}	-0.5805432×10^{0}
2.5	-0.1159641×10^{0}	0.3316134×10^{-1}	-0.4062113×10^{-1}
5.0	-0.4752758×10^{0}	-0.3270653×10^{0}	-0.1777586×10^{0}
7.5	-0.3871634×10^{0}	-0.4264908×10^{0}	-0.4164133×10^{0}
10.0	-0.1546825×10^{0}	-0.2278711×10^{0}	-0.2964029×10^{0}
12.5	0.1084129×10^{-1}	-0.4169627×10^{-1}	-0.1007817×10^{0}
15.0	0.1154036×10^{0}	0.6912151×10^{-1}	0.3343964×10^{-1}
17.5	0.1805450×10^{0}	0.1269958×10^{0}	0.1060608×10^{0}
20.0	0.1766767×10^{0}	0.1943958×10^{0}	0.2040228×10^{0}
22.5	0.2983840×10^{0}	0.2301794×10^{0}	0.1732030×10^{0}
25.0	0.2892486×10^{0}	0.3228513×10^{0}	0.3157561×10^{0}
27.5	0.1229305×10^{0}	0.1809864×10^{0}	0.2413398×10^{0}

In comparison with the results obtained from the integration of 500 divisions (Table 1), we find that the integrated values are, in degree of accuracy, $3\sim5$ digits for $t^*=0\sim2$ and 3 digits for $t^*=18\sim20$.

6. 波源域における津波 [I]

地震研究所　桃井高夫

波源域における津波理論を，解析的にとり扱うことは，非常にむずかしく，もつぱら，数値解析の方法が有力な手段となつている．

二次元の場合に対しては，すでに，比較的波源域の幅が水深に対して，大きい場合について，市栄が，小さい場合には Webb が，それぞれ数値解析を行なつた．そして，三次元の場合における数値解析を行なつたのが，本報告である．

半径 a の内部が，一様にかつ瞬間的に変位したときの発生波の形式的な表現は，すでに佐野—長谷川，あるいは高橋によつて，与えられている．この形式的な積分表示を用い，電子計算機を利用して，近地領域のみの計算を行なつた．計算方法は Simpson の公式にしたがつているが，この積分表示は，被積分函数に，振動項を含むために，Simpson の公式を用いては，あまりに非能率的であり，今後，積分方法を変えて，更に計算を進めるつもりである．

計算結果によると，海底変位をうけた最初の段階での海面変化は，三次元の場合に，長波近似を与えて解いた高橋の近似解と，ほぼ一致する．しかし，次の二点において，少しく相違している．すなわち，

（i） 擾乱域の中心の海面変化で，近似解では，二変と平均海面より上には上らないけれども，数値解によると，中心で平均海面を上下する波が見られる．

（ii） 近似解では，第1の大きな谷が現われるのみであるが，数値解では，第1の谷に続いて，第2，第3，第4，‥‥と小さな谷が次々と現われ，すべて，中心方向に向つて進む．